Unveiling the Dynamic Behavior of Fuzzy Cognitive Maps

Unveiling the Dynamic Behavior of Fuzzy Cognitive Maps

Leonardo Concepción, Gonzalo Nápoles, Rafael Falcon, *Senior Member, IEEE*, Koen Vanhoof and Rafael Bello

***Abstract*—Fuzzy Cognitive Maps (FCMs) are recurrent neural networks comprised of well-defined concepts and causal relations. While the literature about real-world FCM applications is prolific, the studies devoted to understanding the foundations behind these neural networks are rather scant. In this paper, we introduce several definitions and theorems that unveil the dynamic behavior of FCM-based models equipped with transfer F-functions. These analytical expressions allow estimating bounds for the activation value of each neuron and analyzing the covering and proximity of *feasible activation spaces*. The main theoretical findings suggest that the *state space* of any FCM model equipped with transfer F-functions shrinks infinitely with no guarantee for the FCM to converge to a fixed point but to its *limit state space*. This result in conjunction with the covering and proximity values of FCM-based models helps understand their poor performance when solving complex simulation problems.**

***Index Terms*—Fuzzy Cognitive Maps, Recurrent Neural Networks, Non-linear Systems, Shrinking State Spaces.**

I. Introduction

Fuzzy Cognitive Maps (FCMs) [1] [2] continue to grow in popularity because of their flexibility to model complex systems and transparency. In a search carried out in 12/2019, there were over 2000 papers indexed by Scopus, most of them related to applications. A closer inspection on the algorithmic developments in this field reveals that the new proposals are primarily dedicated to learning methods [3] [4] [5] or solving machine learning problems [6] [7] [8]. Other equally relevant theoretical contributions reported in the literature refer to new FCM-like models as illustrated in [9].

Existing theoretical studies on FCMs are mainly devoted to convergence issues. For example, Boutalis et al. [10] studied the existence and uniqueness of fixed points in FCMs equipped with continuous, differentiable transfer functions. Later on, the authors in [11] generalized the findings in [10] by considering the slope parameter of each sigmoid transfer function. However, these theorems have been disproved with numerical counterexamples as explained in [12]. Other results reported in [13] [14] [15] [16] study the convergence of FCM models used in prediction/classification scenarios.

L. Concepción and R. Bello are with the Department of Computer Science, Universidad Central de Las Villas, Cuba. E-mail: {lcperez, rbellop}@uclv.edu.cu

G. Nápoles and K. Vanhoof are with the Faculty of Business Economics, Hasselt Universiteit, Belgium. E-mail: {gonzalo.napoles, koen.vanhoof}@uhasselt.be

G. Nápoles is with the Department of Cognitive Science & Artificial Intelligence, Tilburg University, The Netherlands.

R. Falcon is with the Data Science and Engineering Division, Shopify Inc., Ottawa, Canada and with the School of Electrical Engineering and Computer Science, University of Ottawa, Canada. E-mail: rfalcon@ieee.org

With respect to the theoretical analysis of FCM models and their dynamics, this paper brings two contributions. First, we introduce several definitions and theorems that allow studying the dynamic behavior of FCMs equipped with monotonically increasing functions bounded into non-negative intervals. The strong version of our theorem proves that the state space of an FCM shrinks infinitely and converges to a so-called *limit state space*, which could be a fixed-point attractor in some cases. This allows envisaging, to some extent, the FCM model's behavior prior to the inference stage. As a second contribution, we explore the covering and proximity of *feasible activation spaces*, which help explain why FCMs sometimes perform poorly when solving complex prediction problems. In other words, we show why we should not expect impressive prediction rates when the model has low covering values as the FCM feasible state space is small.

The rest of this paper is organized as follows. Section II goes over the FCM's mathematical underpinnings. Section III introduces important definitions, while Section IV elaborates on the concept of *shrink functions* in FCM-based models. Section V enunciates two theorems that allow unveiling the dynamics behind FCM-based models. Section VI supports the theoretical findings with numerical simulations illustrating why FCM-based models with a reduced number of neurons perform poorly in solving prediction tasks.

II. Fuzzy Cognitive Maps

Concisely speaking, FCMs are knowledge-based recurrent neural networks for modeling complex systems [17]. The FCM topology is denoted by a directed and weighted graph where nodes correspond to neural concepts, while edges represent the causal relations. Unlike traditional neural networks, the FCM topology is often defined by experts in the application domain. The weight $w_{ij} \in [-1, 1]$ denotes the causal influence exerted by neuron C_i upon neuron C_j. The influence may be *excitatory* ($w_{ij} > 0$), *inhibitory* ($w_{ij} < 0$) or *null* ($w_{ij} = 0$). Hence, the weight matrix $W_{M\times M}$ holds the causality information between all pairs of neurons in the graph.

Equation (1) displays the FCM reasoning rule, which resembles the McCulloch-Pitts model [18],

$$A_i^{(t+1)} = f\left(\sum_{j=1}^{M} w_{ji} A_j^{(t)}\right), i \neq j \tag{1}$$

where $A_i^{(t)}$ represents the activation value of the i-th neuron at the t-th iteration step ($t \in \mathbb{N}$), while $f(.)$ denotes the transfer function used to clamp the activation value of a neuron to a

desired interval. The above reasoning rule can be expressed as $f\left(w_i A^{(t)}\right)$ such that $A^{(t)} = (A_1^{(t)}, A_2^{(t)}, \ldots, A_M^{(t)})$ denotes the activation vector and $w_i = (w_{1i}, w_{2i}, \ldots, w_{i-1i}, 0, w_{i+1i}, \ldots, w_{Mi})\ \ \forall i \in \{1, 2, \ldots, M\}$.

The most widely used transfer functions are [19] the *sigmoid* function and the *hyperbolic tangent*. The *bivalent*, *trivalent* and *threshold* functions have also been employed. The former have continuous open intervals as their image set, while the latter have discrete image set (bounded into closed intervals instead). Generally speaking, any bounded and monotonically increasing function over the set of real numbers is a candidate transfer function, since the image set of a bounded function belongs to an interval.

Let F be the set of all monotonically increasing functions bounded into non-negative intervals. Let $F^0 \subset F$ and $F' \subset F$ be the subsets bounded into open intervals and closed intervals respectively. Also, let $f_i \in F$ be the transfer function used in the activation process of neuron C_i (i.e., every neuron has its own transfer function). This means that f_i is bounded into a non-negative interval (either open or closed). In this paper, we refer to an F-function as any function belonging to F.

The reasoning rule displayed in Equation (1) is iteratively repeated until either (i) the FCM converges to a fixed-point attractor or (ii) a maximal number of iterations is reached. The former condition implies that the FCM is stable whereas the latter suggests that it is unstable, and its outputs are either cyclic or completely chaotic. These states can be mathematically defined as follows [17]:

- **Fixed-point** $(\exists t_\alpha \in \{1, 2, \ldots, (T-1)\} : A^{(t+1)} = A^{(t)}, \forall t \geq t_\alpha)$: the map produces the same output after the iteration t_α, so $A^{(t_\alpha)} = A^{(t_\alpha+1)} = A^{(t_\alpha+2)} = \cdots = A^{(T)}$.
- **Limit cycle** $(\exists t_\alpha, P \in \{1, 2, \ldots, (T-1)\} : A^{(t+P)} = A^{(t)}, \forall t \geq t_\alpha)$: the map produces the same output periodically after the period P, so $A^{(t_\alpha)} = A^{(t_\alpha+P)} = A^{(t_\alpha+2P)} = \cdots = A^{(t_\alpha+jP)}$ where $t_\alpha + jP \leq T$, such that $j \in \{1, 2, \ldots, (T-1)\}$.
- **Chaos**: the map continues to produce different state vectors for successive iterations.

III. Theoretical Preliminaries and Definitions

In this section, we introduce some definitions that provide a formal analysis framework to better understand the semantics behind FCM-based models.

Let $\mathcal{L}$ be the set of all non-negative closed intervals and let $\mathcal{S}^M$ be the set of all M-ary Cartesian products over the elements in $\mathcal{L}$. Formally, $\mathcal{S}^M = \{\mathcal{I}_1 \times \mathcal{I}_2 \times \ldots \times \mathcal{I}_M : \mathcal{I}_i \in \mathcal{L}, \forall i = 1, 2, \ldots, M\}$. Every element in $\mathcal{S}^M$ is an M-ary Cartesian product of closed intervals.

Definition 1. *Let $\mathcal{I} \in \mathcal{L}$ and $\mathcal{I}' \in \mathcal{L}$. Interval $\mathcal{I}$ **contains** interval $\mathcal{I}'$ (denoted by $\mathcal{I} \supseteq \mathcal{I}'$) if $\inf(\mathcal{I}) \leq \inf(\mathcal{I}') \wedge \sup(\mathcal{I}) \geq \sup(\mathcal{I}')$. Analogously, interval $\mathcal{I}$ **strictly contains** interval $\mathcal{I}'$ (denoted by $\mathcal{I} \supset \mathcal{I}'$) if $\inf(\mathcal{I}) < \inf(\mathcal{I}') \wedge \sup(\mathcal{I}) > \sup(\mathcal{I}')$.*

Definition 2. *The closed interval $\mathcal{I}_i$ is a **feasible activation space** for the neuron C_i if C_i's activation values always lie inside $\mathcal{I}_i$. Formally, $A_i^{(t)} \in \mathcal{I}_i\ \ \forall t \in \mathbb{N}$.*

Remark. The activation values $A_i^{(t)}$ are confined to the (0,1) interval in sigmoid FCMs, but if a hyperbolic tangent function is used instead, these activation values will lie within (-1,1). We remark that the feasible activation space for a neuron C_i is not unique, therefore multiple feasible activation spaces for the same neuron may exist. If $\mathcal{I}_i$ is a feasible activation space for the neuron C_i, then every closed interval containing $\mathcal{I}_i$ is also a feasible activation space for C_i.

Definition 3. *The closed interval $\mathcal{I}_i$ is the **induced activation space** for neuron C_i if it is the smallest closed interval containing the interval its associated transfer function f_i is bounded to.*

Remark. If $\mathcal{I}_i$ is the induced activation space then, transfer function associated with neuron C_i produces values that always lie inside it. Moreover, if $\mathcal{I}_i'$ contains $\mathcal{I}_i$ then $\mathcal{I}_i'$ is a feasible activation space for C_i.

The following definition extends Definition 2 such that we can refer to specific iterations.

Definition 4. *The closed interval $\mathcal{I}_i^{(t)}$ is a **feasible activation space at t-th iteration** for C_i if activation values for C_i always lies into $\mathcal{I}_i^{(t)}$ at t-th iteration. Formally, the closed interval $\mathcal{I}_i^{(t)}$ is a feasible activation space at t-th iteration for C_i if $A_i^{(t)} \in \mathcal{I}_i^{(t)}$.*

Remark: The 0-th iteration refers to the initial activation values of neurons (input values).

Definition 5. *A **feasible state space** $\mathcal{S}$ is the M-ary Cartesian product over the feasible activation spaces for each map neuron and defined as $\mathcal{S} = \mathcal{I}_1 \times \mathcal{I}_2 \times \ldots \times \mathcal{I}_M$, where $\mathcal{I}_i$ is a feasible activation space for neuron C_i. Formally, $\mathcal{S}$ is a feasible state space if $A^{(t)} \in \mathcal{S}\ \forall t$.*

The aforementioned definition relies on Definition 2 to describe a particular state space of an FCM. Elements in $\mathcal{S}$ are M-tuples, so we have $\mathcal{S} = \mathcal{I}_1 \times \mathcal{I}_2 \times \ldots \times \mathcal{I}_M$ and $A^{(t)} = (A_1^{(t)}, A_2^{(t)}, \ldots, A_M^{(t)})$. Therefore, we can affirm that $\mathcal{S} \in \mathcal{S}^M$. Observe that $A^{(t)} \in \mathcal{S}$ is equivalent to stating that $A_i^{(t)} \in \mathcal{I}_i, \forall i = 1, 2, \ldots, M$.

Definition 3 can be expanded so we can introduce the general notion about the induced activation space.

Definition 6. *The **induced state space** $\mathcal{S}$ is the M-ary Cartesian product over the induced activation spaces for each map neuron and defined as $\mathcal{S} = \mathcal{I}_1 \times \mathcal{I}_2 \times \ldots \times \mathcal{I}_M$, where $\mathcal{I}_i$ is the induced activation space for neuron C_i.*

Also, by means of Definitions 4 and 5 we can define the concept of feasible state space in a specific iteration, which will be a pivotal cornerstone in our theorems.

Definition 7. *A **feasible state space $\mathcal{S}^{(t)}$ at the t-th iteration** is the M-ary Cartesian product over the feasible activation spaces for each map neuron at the t-th iteration and defined as $\mathcal{S}^{(t)} = \mathcal{I}_1^{(t)} \times \mathcal{I}_2^{(t)} \times \ldots \times \mathcal{I}_M^{(t)}$, where $\mathcal{I}_i^{(t)}$ is a feasible activation space at the t-th iteration for neuron C_i. Formally, $\mathcal{S}^{(t)}$ is a feasible state space at the t-th iteration if $A^{(t)} \in \mathcal{S}^{(t)}$.*

Definition 8. *A state space* $\mathcal{S} = \mathcal{I}_1 \times \mathcal{I}_2 \times \ldots \times \mathcal{I}_M$ ***contains*** *state space* $\mathcal{S}' = \mathcal{I}'_1 \times \mathcal{I}'_2 \times \ldots \times \mathcal{I}'_M$ *if* $\mathcal{I}_i$ *contains* $\mathcal{I}'_i$ $\forall i = 1, 2, \ldots, M$. *Formally,* $\mathcal{S} \supseteq \mathcal{S}'$ *(state spaces are sets). Analogously, state space* $\mathcal{S} = \mathcal{I}_1 \times \mathcal{I}_2 \times \ldots \times \mathcal{I}_M$ ***strictly contains*** *state space* $\mathcal{S}' = \mathcal{I}'_1 \times \mathcal{I}'_2 \times \ldots \times \mathcal{I}'_M$ *if* $\mathcal{S}$ *contains* $\mathcal{S}'$ *and* $\mathcal{I}_i$ *strictly contains* $\mathcal{I}'_i$ *for at least one* $i = 1, 2, \ldots, M$. *Formally,* $\mathcal{S} \supset \mathcal{S}'$.

The reader can notice that Definition 8 expands Definition 1 as it goes from real intervals to state spaces. In general, Definitions 1-8 set the ground up by establishing the terminology to be used in the following sections.

IV. Shrink Functions in FCM-based Models

Assuming that $\mathcal{G}$ is the set of all FCMs, let $\mathcal{H}_W : \mathcal{G} \times \mathcal{S}^M \rightarrow \mathcal{S}^M$ and $\mathcal{H}_T : \mathcal{G} \times \mathcal{S}^M \rightarrow \mathcal{S}^M$ be functions that, from an FCM with M neurons and an M-ary Cartesian product of non-negative closed intervals, produce another M-ary Cartesian product of non-negative closed intervals. We refer to $\mathcal{H}_W$ and $\mathcal{H}_T$ as *shrink functions*, which are defined as $\mathcal{H}_W(\mathcal{M}, \mathcal{S}^{(t)}) = \mathcal{S}^{(t+1)}$ and $\mathcal{H}_T(\mathcal{M}, \mathcal{S}^{(t)}) = \mathcal{S}^{(t+1)}$, respectively, such that $\mathcal{M}$ is an FCM and $\mathcal{S}^{(t)} \in \mathcal{S}^M$ $\forall t$.

Both functions take an FCM $\mathcal{M}$ and a feasible state space at the t-th iteration $\mathcal{S}^{(t)}$ for this map and return a feasible state space at the $(t+1)$-th iteration $\mathcal{S}^{(t+1)}$ for the same map. The difference between these functions is that $\mathcal{H}_W$ uses the weight matrix W of $\mathcal{M}$ to calculate a feasible state space for the $(t+1)$-th iteration and $\mathcal{H}_T$ uses the neurons connections (FCM's topology only).

Let $a_j^{(t)}$ and $b_j^{(t)}$ denote the bounds (infimum and supremum respectively) of the closed interval $\mathcal{I}_j^{(t)}$ attached to neuron C_j. Given that $\mathcal{S}^{(t)}$ is a feasible state space at the t-th iteration, the following inequality holds:

$$a_j^{(t)} \leq A_j^{(t)} \leq b_j^{(t)} \ \forall j. \tag{2}$$

As derived from Equation (1), the dot product between w_i and $A^{(t)}$ is computed for every neuron C_i in order to compute its activation value. In this research, we assume that each neuron is influenced by, at least, another neural processing entity. In the case of input neurons, their activation values either remain unchanged or become inactive (depending on the FCM implementation). Whichever the case, their values are easy to predict. Next, we show how to calculate the bounds for the dot product between w_i and $A^{(t)}$.

Case 1: the weight matrix W is unknown. In this case, the minimum value for the dot product is:

$$\min_T \left(w_i A^{(t)} \right) = -\sum_{j=1}^{M} b_j^{(t)} \tag{3}$$

and the maximum value is

$$\max_T \left(w_i A^{(t)} \right) = \sum_{j=1}^{M} b_j^{(t)}. \tag{4}$$

Proof. In order to calculate $\min_T(w_i A^{(t)})$, each map neuron's influence upon C_i (i.e., the product between its activation value and the connection's weight) must be minimal. This is accomplished when the activation value is $b_j^{(t)}$ (maximum) and the weight is -1 (minimum possible value in traditional FCMs). Conversely, to compute $\max_T(w_i A^{(t)})$, each map neuron's influence upon C_i must be maximal, which happens with $b_j^{(t)}$ as activation value and 1 (maximum possible value in traditional FCMs) as the connection's weight. Equations (3) and (4) are obtained after applying this reasoning to every neuron in the map (though only neurons influencing C_i matter, the connection weight for other neurons is 0 and this does not affect the validity of these formulas). ■

Case 2: the weight matrix W is known. In this case, the minimum value for the dot product $w_i A^{(t)}$ is:

$$\sum_{j=1}^{M} \frac{w_{ji} \left(b_j^{(t)}(1 - sgn(w_{ji})) + a_j^{(t)}(1 + sgn(w_{ji})) \right)}{2} \tag{5}$$

and the maximum value is

$$\sum_{j=1}^{M} \frac{w_{ji} \left(b_j^{(t)}(1 + sgn(w_{ji})) + a_j^{(t)}(1 - sgn(w_{ji})) \right)}{2}. \tag{6}$$

Proof. The proof is analogous to the previous case. Aiming at computing $min_W = \min_W (w_i A^{(t)})$, if w_{ji} is negative, then the activation value must be $b_j^{(t)}$ (maximum), thus obtaining $w_{ji} b_j^{(t)}$. But if w_{ji} is not negative then the activation value must be $a_j^{(t)}$ (minimum), thus obtaining $w_{ji} a_j^{(t)}$. Conversely, to calculate $max_W = \max_W (w_i A^{(t)})$, if w_{ji} is negative, then the activation value must be $a_j^{(t)}$, but if w_{ji} is not negative then the activation value must be $b_j^{(t)}$. Equations (5) and (6) above are obtained after applying this reasoning to every neuron in the FCM-based model. In order to achieve both extreme values within a single equation (with no ramifications) we use sign function ($sgn(w_{ji})$). ■

From the monotonically increasing property of $f_i \in F$ (transfer function for neuron C_i), we can state that:

$$a_i^{(t+1)} = f_i\left(min_T\right) \leq A_i^{(t+1)} \leq f_i\left(max_T\right) = b_i^{(t+1)} \ \forall i \tag{7}$$

$$a_i^{(t+1)} = f_i\left(min_W\right) \leq A_i^{(t+1)} \leq f_i\left(max_W\right) = b_i^{(t+1)} \ \forall i \tag{8}$$

In both cases, $\mathcal{I}_i^{(t+1)} = [a_i^{(t+1)}, b_i^{(t+1)}]$ denotes a feasible activation space at the $(t+1)$-th iteration for the neuron $C_i, i = 1, 2, \ldots, M$. Then $\mathcal{S}^{(t+1)} = \mathcal{I}_1^{(t+1)} \times \mathcal{I}_2^{(t+1)} \times \ldots \times \mathcal{I}_M^{(t+1)}$ is a feasible state space at the $(t+1)$-th iteration. This confirms that shrink functions $\mathcal{H}_T$ and $\mathcal{H}_W$ take as inputs an FCM $\mathcal{M}$ and a feasible state space at the t-th iteration for this map and returns a feasible state space at the $(t+1)$-th iteration. Formally, $\mathcal{H}_T(\mathcal{M}, \mathcal{S}^{(t)}) = \mathcal{S}^{(t+1)}$ and $\mathcal{H}_W(\mathcal{M}, \mathcal{S}^{(t)}) = \mathcal{S}^{(t+1)}$.

Overall, we can therefore assert that, over the same FCM, these two shrink functions transform feasible state spaces into state spaces which are also feasible.

V. State Space Estimation in FCM-based Models

In this section we use the definitions formalized above to show that the activation values in FCMs at each iteration are not completely unpredictable.

We know that an FCM's transfer function produces values lying inside an interval (either open or closed). According to Definition 6 we have the induced state space $\mathcal{S}^{(0)} = [a_1^{(0)}, b_1^{(0)}] \times [a_2^{(0)}, b_2^{(0)}] \times \ldots \times [a_M^{(0)}, b_M^{(0)}]$.

In other words, it can be stated that $f_i : \mathbb{R} \to [a_i^{(0)}, b_i^{(0)}]$ or $f_i : \mathbb{R} \to (a_i^{(0)}, b_i^{(0)})$ $\forall i = 1, 2, \ldots, M$. Using the shrink functions $\mathcal{H}_T$ and $\mathcal{H}_W$ for the map $\mathcal{M}$, we can produce feasible activation spaces $\mathcal{S}^{(t+1)}$ from $\mathcal{S}^{(t)}$ $\forall t \in \mathbb{N}$. Inductively, having $\mathcal{S}^{(0)} = [a_1^{(0)}, b_1^{(0)}] \times [a_2^{(0)}, b_2^{(0)}] \times \ldots \times [a_M^{(0)}, b_M^{(0)}]$, then values for $\mathcal{S}^{(1)}, \mathcal{S}^{(2)}, \mathcal{S}^{(3)}, \ldots$ can be obtained.

Theorem 1 (Weak shrinking state space)**.** *In an FCM $\mathcal{M}$, $\mathcal{S}^{(t)}$ contains $\mathcal{S}^{(t+1)}$, $\forall t \in \mathbb{N}$, when state spaces are iteratively calculated using either shrink function $\mathcal{H}_T$ or $\mathcal{H}_W$ with induced state space $\mathcal{S}^{(0)} = [a_1^{(0)}, b_1^{(0)}] \times [a_2^{(0)}, b_2^{(0)}] \times \ldots \times [a_M^{(0)}, b_M^{(0)}]$ and $f_i \in F'$ $\forall i \in \{1, 2, \ldots, M\}$.*

This theorem asserts that the state spaces shrink from one iteration to the next one, although it is possible that $\mathcal{S}^{(t)} = \mathcal{S}^{(t+1)}$, which implies that $\mathcal{S}^{(t)} = \mathcal{S}^{(t+k)}$ $\forall k \in \mathbb{N}$. So, the state spaces may not shrink forever.

Proof. Let $\mathcal{S}^{(t-1)} = \{[a_1^{(t-1)}, b_1^{(t-1)}], \ldots, [a_M^{(t-1)}, b_M^{(t-1)}]\}$, $\mathcal{S}^{(t)} = \{[a_1^{(t)}, b_1^{(t)}], \ldots, [a_M^{(t)}, b_M^{(t)}]\}$ and $\mathcal{S}^{(t+1)} = \{[a_1^{(t+1)}, b_1^{(t+1)}], [a_2^{(t+1)}, b_2^{(t+1)}], \ldots, [a_M^{(t+1)}, b_M^{(t+1)}]\}$.

To prove that $\mathcal{S}^{(t)}$ contains $\mathcal{S}^{(t+1)}$, the fact that $[a_i^{(t)}, b_i^{(t)}]$ contains $[a_i^{(t+1)}, b_i^{(t+1)}]$ for every $i = 1, 2, \ldots, M$ must be demonstrated. Proceeding by induction, let us assume that $\mathcal{S}^{(t-1)}$ contains $\mathcal{S}^{(t)}$ and then prove that $\mathcal{S}^{(t)}$ contains $\mathcal{S}^{(t+1)}$. So, having that $\mathcal{I}_i^{(t-1)}$ contains $\mathcal{I}_i^{(t)}$ for every $i = 1, \ldots, M$, we will prove that $\mathcal{I}_i^{(t)}$ contains $\mathcal{I}_i^{(t+1)}$.

We have that $\mathcal{S}^{(1)}$ is calculated using $\mathcal{S}^{(0)}$, so the induced state space $\mathcal{S}^{(0)}$ contains every state space generated by shrink functions because bounds of $\mathcal{S}^{(0)}$ for every neuron match the transfer function's bounds for this neuron. This implies that $\mathcal{S}^{(0)} \supseteq \mathcal{S}^{(t)}$ $\forall t$, and hence $\mathcal{S}^{(0)}$ contains $\mathcal{S}^{(1)}$.

Case 1: the weights are unknown. The bounds for the dot product between w_i and $A^{(t-1)}$ and between w_i and $A^{(t)}$ are calculated using Equations (3) and (4), respectively.

For all i, we have that:

- $\mathcal{I}_i^{(t)} = [f_i(min_T(w_i A^{(t-1)})), f_i(max_T(w_i A^{(t-1)}))]$
- $\mathcal{I}_i^{(t+1)} = [f_i(min_T(w_i A^{(t)})), f_i(max_T(w_i A^{(t)}))]$.

As the next step, we will prove that the lower bound of $\mathcal{I}_i^{(t)}$ is less than or equal to the lower bound of $\mathcal{I}_i^{(t+1)}$ $\forall i = 1, 2, \ldots, M$. More explicitly,

$$min_T(w_i A^{(t-1)}) \leq min_T(w_i A^{(t)})$$

$$-\sum_{j=1}^{N} b_j^{(t-1)} \leq -\sum_{j=1}^{N} b_j^{(t)}.$$

We should prove that $-b_j^{(t-1)} \leq -b_j^{(t)}$ $\forall j$, which is true because $b_j^{(t-1)} \geq b_j^{(t)}$ by hypothesis ($\mathcal{S}^{(t-1)}$ contains $\mathcal{S}^{(t)}$), so higher bounds of activation space $\mathcal{I}_i^{(t-1)}$ are not smaller than higher bounds for activation space $\mathcal{I}_i^{(t)}$.

Also, let us prove that the upper bound of $\mathcal{I}_i^{(t)}$ is bigger or equal than the upper bound of $\mathcal{I}_i^{(t+1)}$. That is to say,

$$max_T(w_i A^{(t-1)}) \geq max_T(w_i A^{(t)})$$

$$\sum_{j=1}^{N} b_j^{(t-1)} \geq \sum_{j=1}^{N} b_j^{(t)}.$$

By doing so, it is sufficient to prove that $b_j^{(t-1)} \geq b_j^{(t)}$ $\forall j$, which holds by hypothesis.

Case 2: the weights are known. The bounds for the dot product between w_i and $A^{(t-1)}$ and between w_i and $A^{(t)}$ are calculated using Equations (5) and (6), respectively.

Having $\mathcal{S}^{(t)} = \mathcal{I}_1^{(t)} \times \mathcal{I}_2^{(t)} \times \ldots \times \mathcal{I}_M^{(t)}$ and $\mathcal{S}^{(t+1)} = \mathcal{I}_1^{(t+1)} \times \mathcal{I}_2^{(t+1)} \times \ldots \times \mathcal{I}_M^{(t+1)}$, we also know that $\mathcal{I}_i^{(t)} = [f_i(min_W(w_i A^{(t-1)})), f_i(max_W(w_i A^{(t-1)}))]$ and $\mathcal{I}_i^{(t+1)} = [f_i(min_W(w_i A^{(t)})), f_i(max_W(w_i A^{(t)}))]$ $\forall i$.

As the following step, we will prove that the lower bound of $\mathcal{I}_i^{(t)}$ is less than or equal to the lower bound of $\mathcal{I}_i^{(t+1)}$ $\forall i$. Given that f_i is monotonically increasing, it suffices to prove the following inequality:

$$min_W(w_i A^{(t-1)}) \leq min_W(w_i A^{(t)})$$

that is to say

$$\sum_{j=1}^{M} \frac{w_{ji}\left(b_j^{(t-1)}(1 - sgn(w_{ji})) + a_j^{(t-1)}(1 + sgn(w_{ji}))\right)}{2}$$

$$\leq \sum_{j=1}^{M} \frac{w_{ji}\left(b_j^{(t)}(1 - sgn(w_{ji})) + a_j^{(t)}(1 + sgn(w_{ji}))\right)}{2}.$$

It is sufficient to prove that, for every j, that:

$$\frac{w_{ji}\left(b_j^{(t-1)}(1 - sgn(w_{ji})) + a_j^{(t-1)}(1 + sgn(w_{ji}))\right)}{2}$$

$$\leq \frac{w_{ji}\left(b_j^{(t)}(1 - sgn(w_{ji})) + a_j^{(t)}(1 + sgn(w_{ji}))\right)}{2}.$$

There are three possible scenarios depending on the sign of w_{ji}:

- **Scenario 1.** If $sgn(w_{ji}) = -1$ then

  $$\frac{w_{ji}\left(b_j^{(t-1)}(2) + a_j^{(t-1)}(0)\right)}{2} \leq \frac{w_{ji}\left(b_j^{(t)}(2) + a_j^{(t)}(0)\right)}{2}$$

  $$b_j^{(t-1)} w_{ji} \leq b_j^{(t)} w_{ji}$$

  which is true because $sgn(w_{ji}) = -1$ and $b_j^{(t-1)} \geq b_j^{(t)}$ by hypothesis.
- **Scenario 2.** If $sgn(w_{ji}) = 1$ then

  $$\frac{w_{ji}\left(b_j^{(t-1)}(0) + a_j^{(t-1)}(2)\right)}{2} \leq \frac{w_{ji}\left(b_j^{(t)}(0) + a_j^{(t)}(2)\right)}{2}$$

$$a_j^{(t-1)} w_{ji} \leq a_j^{(t)} w_{ji},$$

which is true because $sgn(w_{ji}) = 1$ and $a_j^{(t-1)} \leq a_j^{(t)}$ by hypothesis.

- **Scenario 3.** If $sgn(w_{ji}) = 0$ then the inequality holds because both sides are zero.

Also, let us prove that the upper bound of $\mathcal{I}_i^{(t)}$ is greater than the upper bound of $\mathcal{I}_i^{(t+1)}$ $\forall i$. That is to say,

$$max_W(w_i A^{(t-1)}) \geq max_W(w_i A^{(t)})$$

so,

$$\sum_{j=1}^{M} \frac{w_{ji}\left(b_j^{(t-1)}(1+sgn(w_{ji})) + a_j^{(t-1)}(1-sgn(w_{ji}))\right)}{2}$$

$$\geq \sum_{j=1}^{M} \frac{w_{ji}\left(b_j^{(t)}(1+sgn(w_{ji})) + a_j^{(t)}(1-sgn(w_{ji}))\right)}{2}.$$

It is sufficient to prove that, for every j, that:

$$\frac{w_{ji}\left(b_j^{(t-1)}(1+sgn(w_{ji})) + a_j^{(t-1)}(1-sgn(w_{ji}))\right)}{2} \geq$$

$$\frac{w_{ji}\left(b_j^{(t)}(1+sgn(w_{ji})) + a_j^{(t)}(1-sgn(w_{ji}))\right)}{2}.$$

Analogously to the previous case, there are three possible scenarios depending on the sign of w_{ji}.

- **Scenario 1.** If $sgn(w_{ji}) = -1$ then

$$\frac{w_{ji}\left(b_j^{(t-1)}(0) + a_j^{(t-1)}(2)\right)}{2} \geq \frac{w_{ji}\left(b_j^{(t)}(0) + a_j^{(t)}(2)\right)}{2}$$

$$a_j^{(t-1)} w_{ji} \geq a_j^{(t)} w_{ji}$$

which is true because $sgn(w_{ji}) = -1$ and $a_j^{(t-1)} \leq a_j^{(t)}$ by hypothesis.

- **Scenario 2.** If $sgn(w_{ji}) = 1$ then

$$\frac{w_{ji}\left(b_j^{(t-1)}(2) + a_j^{(t-1)}(0)\right)}{2} \geq \frac{w_{ji}\left(b_j^{(t)}(2) + a_j^{(t)}(0)\right)}{2}$$

$$b_j^{(t-1)} w_{ji} \geq b_j^{(t)} w_{ji}$$

which is true because $sgn(w_{ji}) = 1$ and $b_j^{(t-1)} \geq b_j^{(t)}$ by hypothesis.

- **Scenario 3.** If $sgn(w_{ji}) = 0$ then the inequality holds because both sides are zero.

At this point the thesis is proved for both cases (unknown and known weights) and the theorem is true. ■

Theorem 2 (Strong shrinking state space)**.** *In an FCM $\mathcal{M}$, $\mathcal{S}^{(t)}$ strictly contains $\mathcal{S}^{(t+1)}$, $\forall t \in \mathbb{N}$, when state spaces are iteratively calculated using either shrink function $\mathcal{H}_T$ or $\mathcal{H}_W$ with induced state space $\mathcal{S}^{(0)} = [a_1^{(0)}, b_1^{(0)}] \times [a_2^{(0)}, b_2^{(0)}] \times \ldots \times [a_M^{(0)}, b_M^{(0)}]$ and $f_i \in F^0$ $\forall i \in \{1, 2, \ldots, M\}$.*

Remark. Notice that transfer functions are now bounded into open intervals, which implies that the activation bounds $a_i^{(0)}$ and $b_i^{(0)}$ are never reachable by any neuron C_i at any iteration. This means that $\mathcal{S}^{(t)} \neq \mathcal{S}^{(t+k)}$ $\forall k \in \mathbb{N}$, and hence, the state spaces will shrink forever.

Proof. In order to prove that $\mathcal{S}^{(t)}$ strictly contains $\mathcal{S}^{(t+1)}$, the fact that $[a_i^{(t)}, b_i^{(t)}]$ strictly contains $[a_i^{(t+1)}, b_i^{(t+1)}]$ for every $i = 1, 2, \ldots, M$ must be demonstrated.

Let us assume that $\mathcal{S}^{(t-1)}$ strictly contains $\mathcal{S}^{(t)}$ and then prove that $\mathcal{S}^{(t)}$ strictly contains $\mathcal{S}^{(t+1)}$. So, having that $\mathcal{I}_i^{(t-1)}$ strictly contains $\mathcal{I}_i^{(t)}$ for every $i = 1, 2, \ldots, M$, we will prove that $\mathcal{I}_i^{(t)}$ strictly contains $\mathcal{I}_i^{(t+1)}$.

We have that $\mathcal{S}^{(1)}$ is calculated using $\mathcal{S}^{(0)}$ and applying transfer functions. Then, start of the induction is easily verified and we can affirm that induced state space $\mathcal{S}^{(0)}$ strictly contains every state space generated by shrink functions because bounds of $\mathcal{S}^{(0)}$ for every neuron match transfer function's bounds (open intervals) for this neuron, meaning that $\mathcal{S}^{(0)} \supset \mathcal{S}^{(t)}$ $\forall t$. This happens because between two intervals with equal bounds, the closed one strictly contains the open one. Consequently, $\mathcal{S}^{(0)}$ strictly contains $\mathcal{S}^{(1)}$.

The proof is analogous to the weak version of the theorem, except that all inequalities are turned into strict ones. This means that every occurrence of the $\leq$ and $\geq$ symbols is replaced with the $<$ and $>$ symbols, respectively. Therefore, the strong version of the theorem is true. ■

The above results lead to the question of whether the state spaces will shrink until they reach a single point. Reaching a single point would imply that every feasible activation space has zero length, thus indicating that every FCM converges to a fixed-point attractor. This situation is false, as we know by other studies (e.g., [20], [14], [16]). Such concerns serve as a motivation to define the limit state space.

Definition 9. *$\mathcal{S}^{(\infty)} \in \mathcal{S}^M$ is the **limit state space** of $\mathcal{M}$, when state spaces are iteratively calculated using either shrink function $\mathcal{H}_T$ or $\mathcal{H}_W$ and starting with $\mathcal{S}^{(0)}$, such that $\mathcal{S}^{(\infty)} = \lim_{t\to\infty} \mathcal{S}^{(t)}$.*

It is a fact that, at any iteration, a feasible state space is the M-ary Cartesian product over the feasible activation spaces for each map neuron and that feasible activation spaces are closed intervals over the set of real numbers. The shrinkage of these feasible state spaces implies a shrinkage of the feasible activation spaces. Also, from a mathematical point of view, iterative feasible state spaces are a sequence of elements over $\mathcal{S}^M$ and iterative feasible activation spaces are a sequence of elements over $\mathcal{L}$. A sequence over $\mathcal{L}$ can be interpreted as two other sequences: the sequence of lower bounds and the sequence of upper bounds of the iterative intervals (both sequences are defined over the set of real numbers). We say that a sequence over $\mathcal{L}$ is *convergent*, if the sequences of lower and upper bounds are also convergent.

The theorem implies that closed intervals associated with neurons become smaller from one iteration to the following, meaning that the lower bound becomes bigger and the upper bound becomes smaller. This suggests that the lower bounds sequence increases and the upper bounds sequence decreases. Besides, both sequences are bounded from each other, so the

lower bounds sequence is a lower bound for the higher bound sequence and vice versa. Thus, both sequences are convergent because the *monotone convergence theorem* [21] and have a limit (in the extreme case, the limit is a closed interval with identical lower and upper bounds). Now, we have that the sequence of feasible activation spaces is convergent, implying the convergence of the sequence of feasible state spaces. At this point, there is no doubt about the existence and unicity of a limit for iterative feasible state spaces.

Remark. Even though state spaces do not always shrink until reaching a fixed-point attractor, there are some cases where the limit state space contains a single point as we will observe in the following simulations.

VI. Covering and Proximity of FCM Models

In this section, we discuss two evaluation measures that help understand the properties of FCM-based systems. Such measures are based on the theorems introduced in Section V and the limit state space definition.

A. Evaluation Measures

Definition 10. *The **covering (representativeness) of a feasible activation space at t-th iteration** for neuron C_i is the quotient between the associated interval's length (l_{fas}) and the length of the induced activation space (l_{ias}) for C_i. If neuron C_i is independent, the covering of every associated feasible activation space at any iteration is 0,*

$$covering(\mathcal{I}_i) = \begin{cases} \frac{l_{fas}}{l_{ias}} & \text{if } C_i \text{ has influencing neurons} \\ 0 & \text{if } C_i \text{ has no influencing neurons.} \end{cases}$$

This measure quantifies the proportion of the induced activation space that is reachable by the neuron's activation values. For example, a covering value of 0.2 means that the neuron's activation values reach at most 20% of the induced activation space. A covering of 0 means that at some iteration, the neuron will reach a constant value (because a zero-length interval contains a single value) and will remain there from that point on, regardless of the initial stimulus.

Definition 11. *The **covering of a feasible state space at t-th iteration** $\mathcal{S}^{(t)} = \mathcal{I}_1^{(t)} \times \mathcal{I}_2^{(t)} \times \ldots \times \mathcal{I}_M^{(t)}$, in the FCM $\mathcal{M}$, is the average covering of all feasible activation spaces at t-th iteration $\mathcal{I}_1^{(t)}, \mathcal{I}_2^{(t)}, \ldots, \mathcal{I}_M^{(t)}$. Formally, it is*

$$covering(\mathcal{M}) = \frac{1}{M} \sum_{i=1}^{M} covering(C_i).$$

Analogously to the above example, a covering value of 0.2 means that, on average, every neuron's activation value reaches at most 20% of its induced activation space. We could vaguely say that the tuple $A^{(t)} = (A_1^{(t)}, A_2^{(t)}, \ldots, A_M^{(t)})$ reaches at most 20% of their induced state space. A covering value of zero means that the FCM will reach a fixed-point attractor regardless of the initial stimulus.

Covering is related to the universal approximation property ascribed to multilayer feedforward networks [22]. For instance, suppose we have such a network with a single output neuron whose value lies in $[0, 1]$ and a problem with output values close enough to either 0 or 1. Covering values far from 1 suggest poor approximations to the given input-output set, but values close to 1 do not imply good approximations although they might be good indicators of it.

We know that $\mathcal{S}^{(\infty)}$ is the limit state space of $\mathcal{M}$, but it would be convenient to identify whether $\mathcal{M}$'s activation values lie close to the boundaries established by $\mathcal{S}^{(\infty)}$ or not. The following definitions will help investigate such situations.

Definition 12. *The **proximity (closeness) at the t-th iteration** for neuron C_i, given a feasible activation space for C_i at the t-th iteration, is $proximity(C_i) = \frac{d}{l}$, where d is the smallest distance between its activation value $A_i^{(t)}$ and the boundaries of the activation space and l is the length of the given feasible activation space.*

Remark. The highest proximity value that can be computed is 0.5, which means that the neuron's activation value is near the center of its feasible activation space.

Definition 13. *The **proximity at the t-th iteration** for FCM $\mathcal{M}$, given a feasible state space $\mathcal{S}^{(t)} = \mathcal{I}_1^{(t)} \times \ldots \times \mathcal{I}_M^{(t)}$ at the t-th iteration, is the average proximity of all its neurons given the feasible activation spaces $\mathcal{I}_1^{(t)}, \ldots, \mathcal{I}_M^{(t)}$*

$$proximity(\mathcal{M}) = \frac{\sum_{i=1}^{M} proximity(C_i)}{M}.$$

For example, if $\mathcal{S}^{(t)} = [0.2, 0.6] \times [0.2, 0.6] \times \ldots \times [0.2, 0.6]$ is the given state space for $\mathcal{M}$ and we obtain a proximity value close to 0.5, then it means that the activation values of every neuron are, on average, at the center of the $[0.2, 0.6]$ interval. A proximity value close to 0 suggests that activation values of every neuron are, on average, near to the boundaries of $[0.2, 0.6]$. This measure is not really useful when applied over unstable FCMs because the proximity can easily vary from one iteration to the following.

B. Experimental Scenarios

To illustrate the significance of the theoretical results in this paper, we use covering and proximity measures over the set of synthetically generated FCMs.

For experimentation purposes, we generated 400 FCM-based models (200 stable and 200 unstable). The number of neurons is randomly generated and may vary between 5 and 30, whereas weights are uniformly distributed in the $[-1, 1]$ interval. Such cognitive networks are generated with different connectivity or percentage of relationships (10%, 20%, ..., 100%) but self-connections are not allowed.

Moreover, we generated 20 initial state vectors such that each record comprises an initial stimulus and the expected response after 100 iterations, where neuron activation values are randomly distributed in $[0, 1]$. Responses associated with every stimulus are calculated using the sigmoid transfer function $f(x) = 1/(1 + e^{-\lambda(x-h)})$, such that λ and h are positive numbers randomly selected for each case. Discrete functions (bivalent, trivalent and threshold) could be used because they are compatible with our theorems. However, we decided to

exclude them from the experiments based on the findings in [20] related to their inference capabilities.

Observe that the generated FCMs correspond to simulation problems in which each concept can be regarded as either an input or output variable. FCM-based models used for pattern classification are neglected due to two main reasons. Firstly, in our previous papers [13] [14] [15] [16], the issues related with FCM-based classifiers have been widely discussed. Secondly, the literature reports notably fewer FCM solutions for pattern classification problems as they regularly perform poorly when compared with traditional classifiers.

For each synthetic FCM model, we calculate two feasible state spaces $\mathcal{S}^{(t)}$ at the t-th iteration: one using the $\mathcal{H}_W$ shrink function (i.e., knowing the weight matrix) and the other using the $\mathcal{H}_T$ function (i.e., only knowing the FCM's topology). For each feasible state space, we calculate the FCM model's covering and proximity. We remark that all FCMs employ the sigmoid function as their transfer function, which belongs to F^0 because it is bounded into $(0, 1)$. Applying the *Strong Shrinking State Space Theorem*, we obtain that $A^{(t)} \in \mathcal{S}^{(t)}$. Due to the difficulty of mathematically computing $\mathcal{S}^{(\infty)}$, we opt by a computational approach. In the following experiments we set $T = 100$, hence we calculate $S^{(T)}$ using both $\mathcal{H}_W$ and $\mathcal{H}_T$. From now on, we divide the experiments according to: (i) their FCM stability features and (ii) the shrink function used to calculate the feasible state spaces.

In the generated FCM models, we analyze the influence of several factors such as number of neurons, connectivity, stability and the shrink function ($\mathcal{H}_W$ or $\mathcal{H}_T$) upon the final results in terms of covering and proximity. Connectivity is the ratio of the number of causal relations among neurons to the maximum number of such possible relations in the FCM. Also, we provide an interpretation for the obtained values of covering and proximity while paying attention to the number of iterations needed for the convergence of every state space to the limit state space (i.e., not the theoretical definition but its computational approximation).

1) Unstable FCMs and $\mathcal{H}_T$ shrink function: This function makes no use of the FCM weights, so we assume that weights range within $[-1, 1]$. This means that results are more general and hence applicable to every FCM with the same topology. Yet the calculated feasible state spaces are wider than those calculated using the weight matrix.

Fig. 1 depicts the results for the unstable FCMs obtained in our numerical simulations. Regardless of the number of neurons or connectivity, covering values are always very high. Moreover, we gathered computational evidence that every FCM reaches the limit state space before the 100-th iteration (on average only 10 iterations were needed), which suggests that the calculated feasible state spaces are good computational approximations of the limit state spaces.

Fig. 2 portrays the distribution of covering values for unstable FCMs. From this experiment we cannot draw meaningful conclusions, in spite of the high covering values reported for these maps. In a nutshell, the FCMs' instability and lack of knowledge about weights when computing the feasible state spaces render these estimated feasible state spaces unable to bear any predictive information.

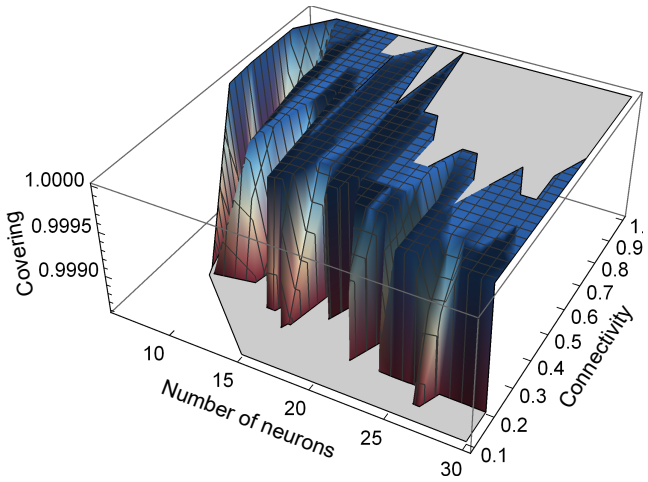

Fig. 1: Covering values for unstable FCM models using the $\mathcal{H}_T$ shrink function.

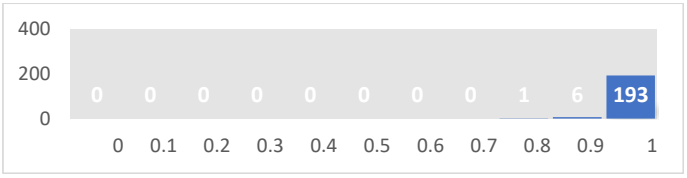

Fig. 2: Distribution of covering values among the unstable FCMs using the $\mathcal{H}_T$ shrink function.

2) Unstable FCMs and $\mathcal{H}_W$ shrink function: An awareness of the matrix W leads to better results in the sense that feasible state spaces are more compact. It can be noticed from Fig. 1 that higher connectivity values mean higher covering values and that the number of neurons appears to have no significant influence on the covering values. The covering value is 1 in almost every case when the number of neurons is higher than 15 and the connectivity is higher than 0.5. Also, we realized that 178 FCMs reached the limit state space before the 100-th iteration (on average we required 58 iterations), which is an indicator of good computational approximations.

Fig. 3 displays the distribution of covering values for this scenario. Notice that there are some FCMs with small covering values, which confirm that weights help estimate small feasible state spaces where these activation values belong, even in the case of unstable FCM-based models.

Overall, unstable FCMs rarely have small covering values (regardless of the use of the causal weights in the calculations) because the activation values of neurons constantly change without understandable patterns.

3) Stable FCMs and $\mathcal{H}_T$ shrink function: In this experiments, both covering and proximity values are shown because these FCMs do reach stable states, hence these values remain almost unchanged toward the last iterations.

According to Fig. 4 it can be concluded that higher connectivity values lead to higher covering values and that the number of neurons in the network has no significant influence on the covering values. Of course, in real FCM-based models, we can expect a straightforward relation between the number

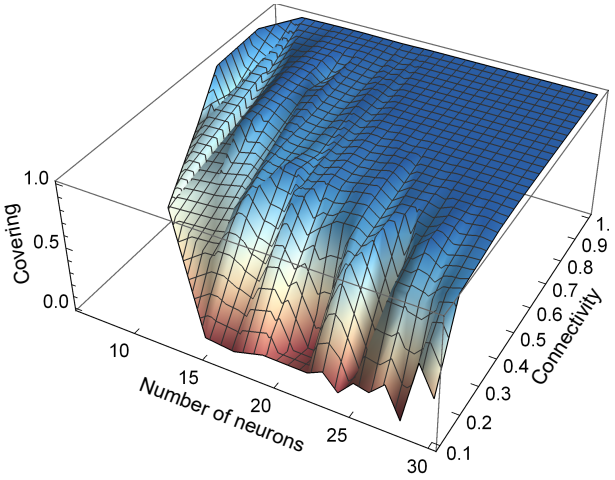

Covering values for unstable FCM models using the $\mathcal{H}_W$ shrink function.

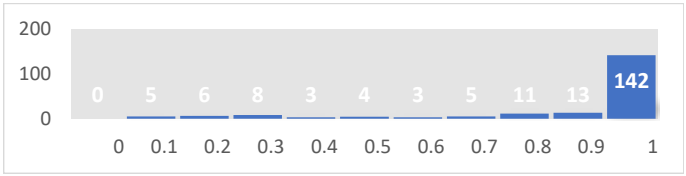

Fig. 3: Distribution of covering values for unstable FCMs using the $\mathcal{H}_W$ shrink function.

of neurons and the connectivity.

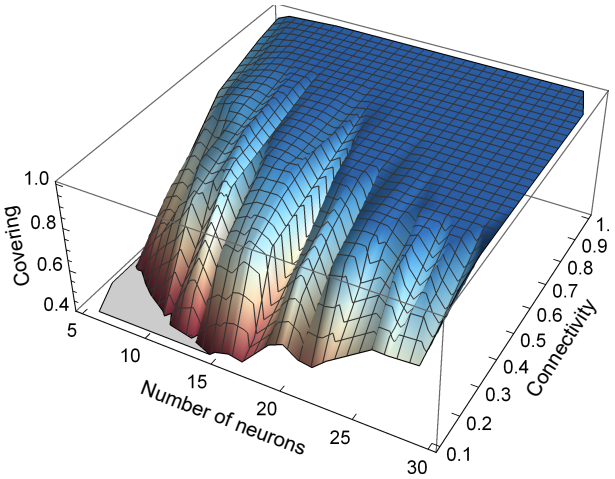

Fig. 4: Covering values for stable FCM models using the $\mathcal{H}_T$ shrink function.

Fig. 5 discloses the distribution of covering values for this scenario. Covering value reaches 1 in almost every case when connectivity is higher than 0.6. Moreover, every FCM reaches the limit state space before the 100-th iteration (on average only 12 iterations were needed).

It can be observed that the lack of knowledge about the weights significantly diminishes our capacity to estimate informative state spaces. The results also illustrate that there are some FCMs with small covering values, which implies that

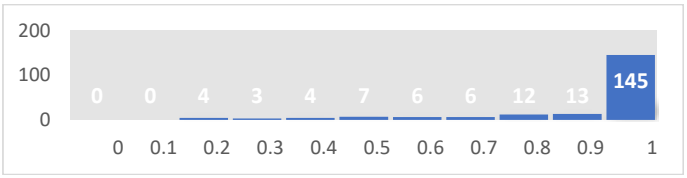

Fig. 5: Distribution of covering values for stable FCMs using the $\mathcal{H}_T$ shrink function.

our experiment helps estimate small feasible state spaces to which the activation values belong, even when only the FCM topology is known. Overall, an FCM-based model with a small covering value for a fixed topology implies that, regardless of the weight matrix, the covering will be less than or equal to the one without considering the weights. Thus, if we obtain zero covering with a fixed topology, every FCM matching this topology will converge to a fixed-point attractor.

Fig. 6 shows the distribution of proximity values for this scenario. According to this figure, almost every proximity value lies between 0.2 and 0.4. Only 8 FCMs have proximity values below 0.2, which means that, in general, the activation values are not close to the boundaries of the corresponding activation spaces. On the other hand, notice that the activation values do not commonly lie in the middle of the activation spaces because only 12 FCMs are nearby.

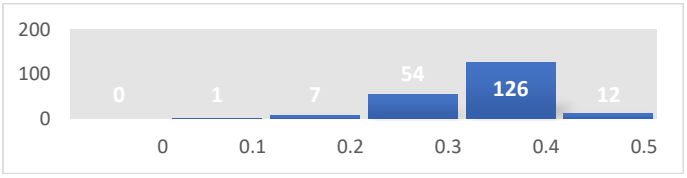

Fig. 6: Distribution of proximity values for stable FCMs using the $\mathcal{H}_T$ shrink function.

Based on the results of both measures (covering and proximity) we can conclude that the predicted state spaces are not good enough approximations of the real activation values when the knowledge about weights is not available, even in presence of FCM models to converge to a fixed point.

4) Stable FCMs and $\mathcal{H}_W$ shrink function: Fig. 7 shows the covering values resulting for this scenario. The results have shown that higher connectivity values and higher number of map neurons do have a considerable influence on attaining higher covering values. In the current experiment, 149 FCMs reached the limit state space before the 100-th iteration (on average 57 iterations were needed), which confirms the usefulness of the calculated feasible state spaces to approximate the limit state spaces.

Being more explicit, note that covering values are regularly near to 1 when the connectivity is higher than 0.6. We obtained zero covering for almost every FCM with connectivity 0.2 or under (about 20% of the neuron pairs are connected, which means that every neural entity is connected to 1 in 5). We also have zero covering for almost every FCM-based model with 10 neurons or less. This result is very important in the FCM

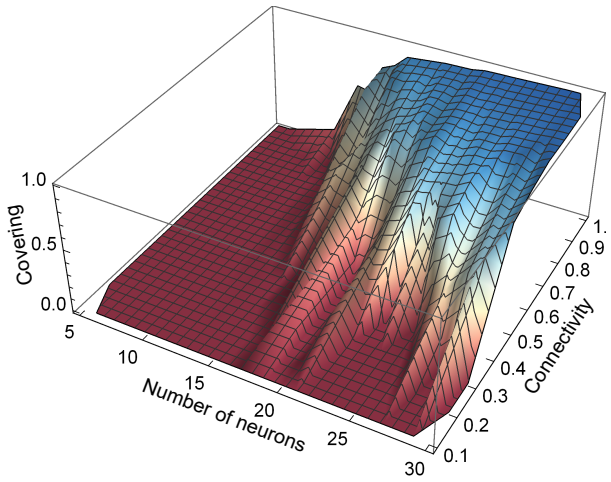

Fig. 7: Covering values for stable FCM models using the $\mathcal{H}_W$ shrink function.

field, since most real-world models usually involve topologies with a limited number of neurons. By calculating covering we can peek at the FCM's behavior without running the inference process, so we could notify the expert about the limitations of the FCM model to reach good approximations.

Now with stable FCMs and the knowledge of causal weights in the calculations, we obtain predictive information about the FCM's behavior. As already discussed, the covering value for every FCM is the average covering for every neuron. Hereby, a zero covering value is a computational evidence of fixed-point attractors for every one of these FCM models. This implies that, regardless of the initial stimulus, the FCM will always converge to a fixed-point attractor, and Fig. 8 illustrates that at least 81 FCMs obey this pattern.

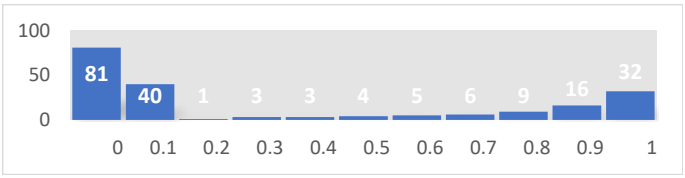

Fig. 8: Distribution of covering values for stable FCMs using the $\mathcal{H}_W$ shrink function.

Fig. 8 reveals that 121 FCMs have small covering values (between 0 and 0.1), thus we can estimate small feasible state spaces to which these activation values belong. We generate datasets consisting of 20 input-output pairs to analyze these FCMs from the accuracy point of view. Accuracy is defined as the average of (always positive) differences between expected outputs and activation values at the last iteration. Also, using the limit state space for each FCM, we can compute the best possible accuracy that could be achieved with a specific dataset by means of the distance of the outputs to the neurons' activation space. After this testing, we discovered that the average of all best possible accuracies is around 0.272. This outcome, obtained before starting the inference process, means that we cannot expect better results than 0.272 on average. Actually, we empirically confirmed this conclusion by getting an average accuracy of 0.275. We can see how low covering is associated to poor performance in FCM-based models.

Despite these encouraging results, some FCMs escape the orbit of our math and we cannot narrow down their state spaces. Perhaps some state spaces cannot be tighter than what we estimated and the FCMs converge to different fixed-point attractors, which could be widely spread along the induced state space. While the literature reports some FCM-based scenarios on which unique fixed points are convenient, the truth is that the convergence to different fixed-point attractors is a pivotal feature to produce heterogeneous responses in a stable way. Therefore, we should avoid zero covering in FCMs when we need diverse responses.

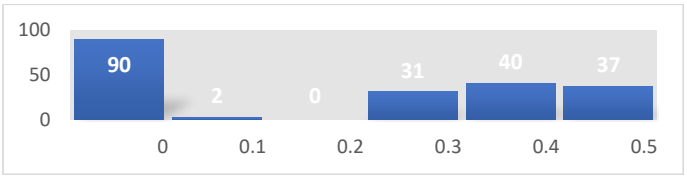

Fig. 9: Distribution of proximity values for stable FCMs using the $\mathcal{H}_W$ shrink function.

According to Fig. 9, nearly half of the proximity values are exactly zero. So, almost surely, 90 FCMs converge to a fixed-point attractor (regardless of their initial stimulus vector). It is almost surely because, when a stable FCM has 0 valued proximity, it means the activation value for every neuron at any high enough iteration will match the lower or higher bound of predicted feasible activation state for current iteration. This is highly unlikely, except if every feasible activation state has length 0. This last situation implies that covering is 0 and then the FCM converges to a fixed-point attractor. In this case, the activation intervals for FCMs are not as wide as in previous cases and the current results must be carefully interpreted. For example, a proximity of 0.5 means that, on average, the actual activation values lie in the middle of the activation space. However, for an specific neuron, this does not imply that its activation is far from the boundaries because the length of the activation space could be approaching zero.

In stable FCMs and using weights in our calculations, we conclude that combining the results of both evaluation measures, the predicted state spaces are good enough approximations of the real activation values in many cases. Moreover, by means of the *Strong Shrinking State Space Theorem*, we gathered computational evidence about the convergence to a fixed-point attractor in such maps.

C. Discussion of Simulation Results

In many situations (e.g., pattern recognition), stable FCMs with covering values close to 1 (high representation ability) and proximity values close to 0 (high accuracy) are regularly desired. In other situations, like control scenarios (where a goal may be to produce the same response despite the activation vector used to activate the map), covering values close to 0 are sought-after. The simulations reported more valuable results in

the presence of stable FCM models and when the knowledge comprised into the weight set is available.

In our experiments, we obtained high covering values for the case of unstable FCMs and when we only take their topology into account. In this case, the feasible activation spaces are not a narrow representation of the real activation values, as we can observe from the high proximity values in the results. Also, we conclude that there is not such chaos in every unstable FCM, because sometimes their activation values reside within small activation spaces (see Fig. 3).

The results confirmed that the predictive information about the system is found by working with stable maps and their weight sets. Small covering values are evidence of the reduced representativeness of induced activation space, but sometimes we desire high covering values to represent the most diverse sets of outputs. The last scenario has proven useful to predict the FCMs' behavior (e.g., fixed-point attractors) by means of covering and proximity values. As illustrated, such measures have a straightforward connection with the *Strong Shrinking State Space Theorem*. More importantly, they help explain why FCMs sometimes perform poorly when applied to prediction problems that demand high accuracy. Having a low covering value means there is a vast state space region where no FCM responses lie in. In this situation, it is more likely to have desired responses residing into the aforementioned region. Such responses will never be reached by the FCM in question, hence substantially reducing its accuracy.

VII. Concluding Remarks

In this paper, we have introduced a theoretical formalism consisting of definitions and theorems to unveil the dynamical behavior of FCMs equipped with transfer F-functions. To the best of our knowledge, similar studies reported in the literature focus on the existence and unicity of the fixed-point attractor. Our research however goes a step further since it analyses the dynamical behavior of FCM-based models from the perspective of their state spaces.

The *Strong Shrinking State Space theorem* enunciated in this paper ensures that the feasible state space of an FCM-based system equipped with a tranfer F-function shrinks infinitely, yet the system converges to its limit state space. As shown in the experiments, approximating an FCM's limit state space is useful to predict fixed-point attractors. This is consistent with the notions of E-stability and E-instability proposed by Nápoles et al. [16]. Likewise, we illustrated that the covering of feasible activation spaces is often poor and irregular for FCMs with reduced network topologies. This knowledge could be injected into the learning procedure in order to improve network's performance. Of course, it is not expected of FCM-based models to fulfill the universal approximation property due to their lack of hidden neurons and the fact that both weights and neurons' activation values are bounded. As a future work, we will use our results to improve the prediction capability of FCM-based models.

References

[1] B. Kosko, "Fuzzy cognitive maps," *International Journal Man-Machine Studies*, vol. 24, no. 1, pp. 65–75, 1986.

[2] ——, "Hidden patterns in combined and adaptive knowledge networks," *International Journal of Approximate Reasoning*, vol. 2, no. 4, pp. 377–393, 1988.

[3] K. Wu and J. Liu, "Learning large-scale fuzzy cognitive maps based on compressed sensing and application in reconstructing gene regulatory networks," *IEEE Transactions on Fuzzy Systems*, vol. 25, no. 6, pp. 1546–1560, 2017.

[4] J. Salmeron, T. Mansouri, M. Moghadam, and A. Mardani, "Learning fuzzy cognitive maps with modified asexual reproduction optimisation algorithm," *Knowledge-Based Systems*, vol. 163, pp. 723–735, 2019.

[5] Z. Yang and J. Liu, "Learning of fuzzy cognitive maps using a niching-based multi-modal multi-agent genetic algorithm," *Applied Soft Computing*, vol. 74, pp. 356–367, 2019.

[6] W. Pedrycz, A. Jastrzebska, and W. Homenda, "Design of fuzzy cognitive maps for modeling time series," *IEEE Transactions on Fuzzy Systems*, vol. 24, pp. 120–130, 2016.

[7] W. Froelich and W. Pedrycz, "Fuzzy cognitive maps in the modeling of granular time series," *Knowledge-Based Systems*, vol. 115, pp. 110–122, 2017.

[8] W. Homenda and A. Jastrzebska, "Clustering techniques for fuzzy cognitive map design for time series modeling," *Neurocomputing*, vol. 232, pp. 3–15, 2017.

[9] W. Froelich and J. L. Salmeron, "Advances in fuzzy cognitive maps theory," *Neurocomputing*, pp. 1–2, 2017.

[10] Y. Boutalis, T. L. Kottas, and M. Christodoulou, "Adaptive estimation of fuzzy cognitive maps with proven stability and parameter convergence," *IEEE Transactions Fuzzy Systems*, vol. 17, no. 4, pp. 874–889, 2009.

[11] T. Kottas, Y. Boutalis, and M. Christodoulou, "Bi-linear adaptive estimation of fuzzy cognitive networks," *Applied Soft Computing*, vol. 12, no. 12, pp. 3736–3756, 2012.

[12] I. Á. Harmati, M. F. Hatwágner, and L. T. Kóczy, "On the existence and uniqueness of fixed points of fuzzy cognitive maps," in *Information Processing and Management of Uncertainty in Knowledge-Based Systems. Theory and Foundations*, J. Medina, M. Ojeda-Aciego, J. L. Verdegay, D. A. Pelta, I. P. Cabrera, B. Bouchon-Meunier, and R. R. Yager, Eds. Springer International Publishing, 2018, pp. 490–500.

[13] G. Nápoles, R. Bello, and K. Vanhoof, "How to improve the convergence on sigmoid fuzzy cognitive maps?" *Intelligent Data Analysis*, vol. 18, no. 6S, pp. S77–S88, 2014.

[14] G. Nápoles, E. Papageorgiou, R. Bello, and K. Vanhoof, "On the convergence of sigmoid fuzzy cognitive maps," *Information Sciences*, vol. 349-350, pp. 154–171, 2016.

[15] ——, "Learning and convergence of fuzzy cognitive maps used in pattern recognition," *Neural Processing Letters*, vol. 45, pp. 431—-444, 2017.

[16] G. Nápoles, L. Concepción, R. Falcon, R. Bello, and K. Vanhoof, "On the accuracy-convergence tradeoff in sigmoid fuzzy cognitive maps," *IEEE Transactions on Fuzzy Systems*, vol. 26, no. 4, pp. 2479–2484, 2018.

[17] G. Felix, G. Nápoles, R. Falcon, W. Froelich, K. Vanhoof, and R. Bello, "A review on methods and software for fuzzy cognitive maps," *Artificial Intelligence Review*, pp. 1–31, 2017.

[18] L. Zhang and B. Zhang, "A geometrical representation of mcculloch-pitts neural model and its applications," *IEEE Transactions on Neural Networks*, vol. 10, no. 4, pp. 925–929, 1999.

[19] S. Bueno and J. L. Salmeron, "Benchmarking main activation functions in fuzzy cognitive maps," *Expert Systems with Applications*, vol. 36, no. 3, pp. 5221–5229, 2009.

[20] A. K. Tsadiras, "Comparing the inference capabilities of binary, trivalent and sigmoid fuzzy cognitive maps," *Information Sciences*, vol. 178, no. 20, pp. 3880–3894, 2008.

[21] K. G. Binmore, *Mathematical Analysis: A Straightforward Approach*. Cambridge University Press, 1977.

[22] K. Hornik, M. Stinchcombe, and H. White, "Multilayer feedforward networks are universal approximators," *Neural Networks*, vol. 2, pp. 359–366, 1989.